

# Experimental research on flow field of a high head model pump turbine based on PIV test

Demin Liu (✉ [liudemin999@126.com](mailto:liudemin999@126.com))

Dongfang electric machinery CO.,LTD

Yongzhi Zhao

Dongfang electric company

Weilin Xu

Sichuan University

---

## Original Article

**Keywords:** pump turbine, PIV, Pressure fluctuation, Pump hump, Cavitation, Four quadrants curve working points

**Posted Date:** March 31st, 2020

**DOI:** <https://doi.org/10.21203/rs.3.rs-19924/v1>

**License:** © ⓘ This work is licensed under a Creative Commons Attribution 4.0 International License.

[Read Full License](#)

---

## Experimental research on flow field of a high head model pump turbine based on PIV test

LIU Demin<sup>1,2,\*</sup>, XU Weilin<sup>1</sup>, and ZHAO Yongzhi<sup>2</sup>

*1 Sichuan University, Chengdu 610065, Sichuan Province, P.R. China.*

*2 Dongfang Electric Machinery Co., Ltd, Deyang 618000, China*

Received March 28, 2020; revised May 12, 2020; accepted August 12, 2020

**Abstract:** Pump turbine operating conditions are complex, mainly including turbine mode and pump mode. Pump turbines have various instability problems during operation, such as S-shaped, pump hump, pressure pulsation and cavitation. PIV (Particle Image Velocimetry) is a very effective test technique for the internal flow field observation of pump turbines. In this paper, the internal flow field of pump hump, cavitation, pressure pulsation and four quadrants of the pump turbine are tested by PIV technology. The experimental observations show that the internal flow on those unstable working conditions of the pump turbine is extremely complicated. Those conditions which the vortex separation is serious and the flow angle is changed is far away the best efficiency working condition. Since the operating condition deviates from the optimal operating condition, the inflow Angle is changed and the inflow Angle is far away from the optimal inflow Angle. And the vortex induces and develops strongly by PIV test. The flow phenomenon are demonstrated at each operating points by PIV test.

**Keywords:** pump turbine, PIV, Pressure fluctuation, Pump hump, Cavitation, Four quadrants curve working points

### 1 Introduction

Developing clean energy and supporting sustainable social development are the strategic goals of China's energy industry. According to the energy composition of China in 2018 as shown in Fig.1, about 2/3 of the current electricity still comes from coal-fired power generation [1], which brings great pressure on China to achieve the social development goals such as greenhouse gas emission reduction and air pollution reduction.

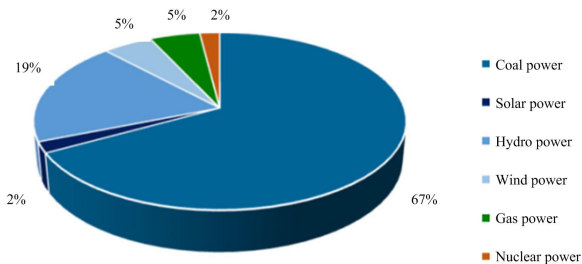


Fig. 1. Ratios of different power generation in China

At the same time, in recent years, wind power, photovoltaic power and other renewable energy have been developing rapidly, and their proportion in the power

market has been increasing year by year, which also makes the stability of China's power system face severe challenges. Therefore, it is an important strategy to develop hydro-power, especially large capacity pumped storage, and enhance the ability of rapid adjustment of the whole power system.

Fig.2 lists the design heads of pumped storage power stations at home and abroad since the 1960s[2], which fully illustrates the trend of modern pumped storage technology towards the direction of high head and large capacity. Some the large pumped storage power stations built or under construction in China have water heads over 700m such as Changlongshan and Dunhua project of China. High head pumped storage technology not only puts forward higher requirements on the structure of power plant units, but also emphasizes more on the operation quality of units when they deviate from the design working point.

Existing studies have shown that when the operation deviates from the design condition, unsteady and unstable flow phenomena often occur in the pumped storage unit. Pump in low load condition is easy to have the strong water pressure pulsation and the pressure pulsation can be

\* Corresponding author. E-mail: liudemin999@126.com

Supported by National Natural Science Foundation of China (No.51279172) and Deyang funded science and technology support program (2018CKJ002)

induced by intermittent cavitation<sup>[3-4]</sup>. And the uneven pressure pulsation is the main reason of hydraulic radial force fluctuations, the instability of rotor dynamics<sup>[5]</sup>, serious intense vibration<sup>[6]</sup>, crack of crown fracture and runner<sup>[7]</sup>. What is more serious is that the safe operation of the unit will be affected.

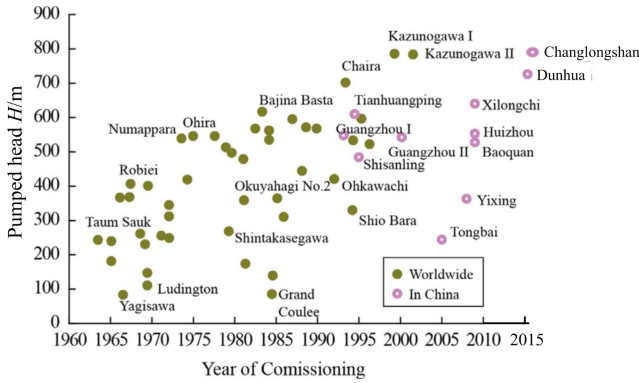


Fig. 2. Pumping head variations for pumped storage power-stations<sup>[2]</sup>

Pump turbine needs two-way operation, both pump and turbine working mode, operating conditions throughout the pump, pump brake, turbine, turbine brake, reverse pump five operating conditions, the operating conditions are complex and variable. The hydraulic development of pump turbine must meet both the performance requirements of turbine and pump, and the transient transition process characteristics must be considered between different working conditions.

The strong pressure pulsation under the pump working condition of pumped storage unit is caused by the rotor-stator interference between the runner and the movable guide vane. The strong vortex at the inlet of the movable guide vane near the lower ring of the runner causes the counter-current in the guide vane, which makes the flow in the guide vane passage go through the periodic cycle of unobstructed -- blocked -- counter-current -- blocked -- unobstructed<sup>[8]</sup>. This cyclic process leads to a sharp increase in the hydraulic loss in the guide vane, which is then reflected in the hump of the performance curve or characteristic curve<sup>[7]</sup>.

Because the hump of the performance curve or characteristic curve is the external manifestation of the instability of the internal flow of hydraulic rotating machinery, it is an inevitable way to further develop the pumped storage technology to put forward the engineering strategy of suppressing the hump by studying

the mechanism of the internal instability flow.

Although the study of hump phenomenon history can be traced back to the 1970s, but still needs further comb existing research data to clearly reveal pumped storage unit pump working conditions of unstable flow characteristics, and based on the fundamental properties of the internal flow unit to determine reasonable engineering measures to suppress the hump phenomenon, thus enhancing the running stability of the unit.

Fig.3 shows the characteristic curve of pump operating condition under certain operating degree of pumped storage unit measured by model test<sup>[9]</sup>. The abscissa represents the dimensionless flow compared with the optimal efficiency point flow (QBEP), and the ordinate represents the dimensionless flow compared with the optimal efficiency point head. In the Fig.3, there are two humps in the vicinity of 0.90QBEP and 0.70QBEP, which are respectively represented by PS1 and PS2.

From the results in Fig.3, it can be seen that the operating condition range and corresponding pressure pulsation of the hump are different when the experiment is carried out in different flow regulation directions. This phenomenon is called delay phenomenon. However, in the results shown in Fig.3, the delay phenomenon corresponding to the two flow directions is not significant.

According to the<sup>[9]</sup> research, no matter in the direction of small flow to large flow or from large flow to small flow, the pressure pulsation in the working conditions around the hump PS2 (such as point B) is more intense than that around the working conditions around the hump PS1 (such as point A).

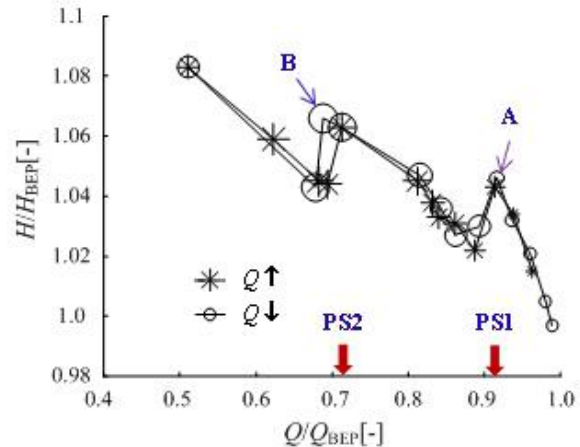


Fig. 3. Positive slope at characteristic curve for pumped storage unit at pump mode

Unsteady CFD methods for simulating the amplitudes and frequencies of pressure fluctuations of pump turbines have been widely used, and RANS method is most popular among them. Unsteady simulations in normal operating condition were developed [10-12], and the results showed that for the monitoring point closest to the runner, maximum pressure amplitude is observed for the same component, indicating the strong influence of the potential effect in the interactions between the guide vanes and the rotating runner blades. The amplitude of this component decreases very fast backward to the stay vanes. Other studies simulated the off-design operating condition to investigate different feature of pressure fluctuations. Yan [13] simulated the hydrodynamics in a pump-turbine at off-design operating conditions in turbine mode and found that the low frequency components appear at runaway and low discharge conditions. Widmer[14] did similar simulation and found that during unsteady vortex formation, the vortices in the runner and the vaneless space fluctuate in time, and induce in-phase pressure fluctuations in the vaneless space. Yin [15] predicted pressure fluctuations under low partial flow of pump mode and suggested that the low frequency pressure fluctuations are essential. Xiao [16] and Liu[17] simulated the unsteady flow within the entire flow passage of a pump-turbine with misaligned guide vanes (MGV). Three arrangements of MGV of different opening angles were chosen to analyze the influence of MGV on the pressure pulsations and four quadrants curve. It was found that by using the MGV, the four quadrants curve shape is improved and the fluctuation amplitudes close to the synchronous opening guide vanes have been reduced significantly.

## 2 Experiment

### 2.1 PIV parameter on pump-turbine

The research object is a reduced pump-turbine, and the whole model includes the draft tube, impeller, guide vane, stay vane and spiral case, as shown in Fig. 4. The number of impeller blades is 9 and the number of guide vanes is 22, as listed in Table 1.

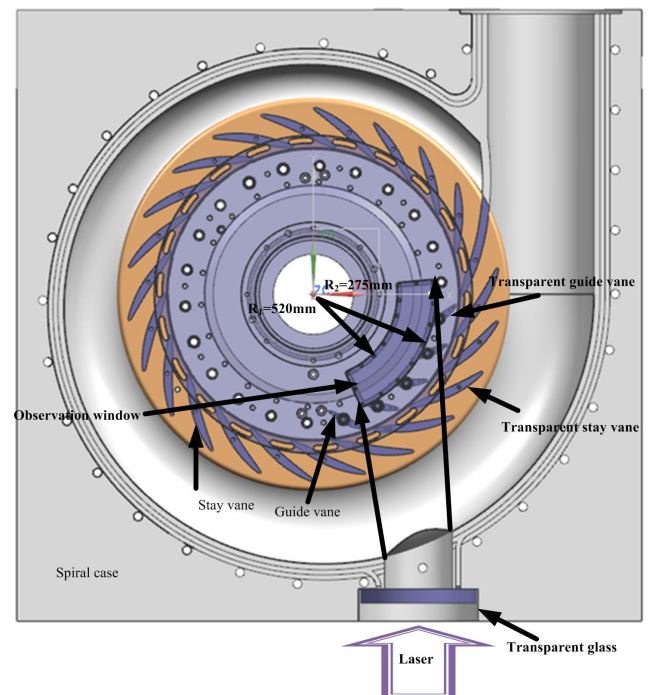
**Table 1.** Main parameters of the tested pump-turbine model.

Impeller diameter at inlet $D_1$ / mm	530
Impeller diameter at outlet $D_2$ / mm	250
Impeller blade number $Z_1$	9
Guide vane number $Z_0$	22
Rated guide vane opening $a/(^\circ)$	20

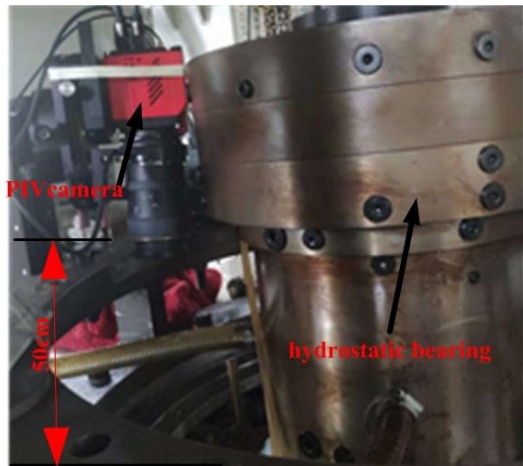
Rotational speed $N/(r/min)$	900
Height of guide vane $b_0/mm$	37.6
specific speed $ns=np^{0.5}/H^{1.25}$	93

### 2.2 PIV structure on pump-turbine

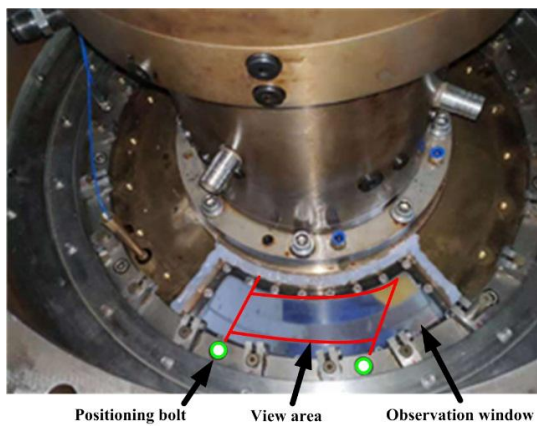
The test device design the observation window on the headcover of model pump turbine, and the PIV camera is loaded on the top of the headcover to capture the fluid motion state under the observation window. A window is designed on one side of the volute to ensure that the laser emitted by the PIV laser enters the fluid, and the laser passes through the transparent fixed guide vane and the movable guide vane and enters the location of the vane-less area between the guide vane and the impeller. In order to ensure the shooting effect, transparent Windows are made of acrylic plexiglass. In order to ensure the transparency of movable guide vane and fixed guide vane, the manufacturing of guide vane must adopt water grinding technology to ensure the processing accuracy and transparent. The laser beam passes through the fixed guide vane and the movable guide vane along the transparent window of the volute. In order to ensure the objectivity of test results, test parameters is 40m water head according to IEC regulations, and the transparent window must bear the minimal pressure of 0.5Mpa.



(a) Pump turbine structure for PIV test



(b) PIV camera



(c) Transparent window and view area

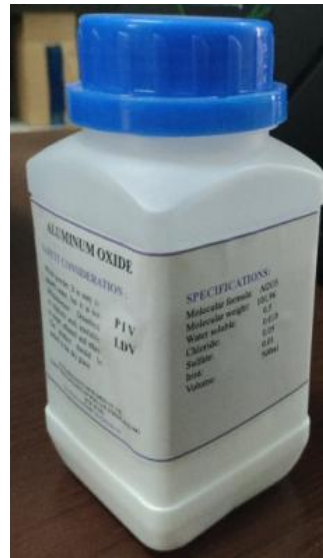
**Fig.4.** The structure of the pump-turbine model.

The main test instruments include PIV laser, PIV camera, and model pump turbine and so on, as shown in Fig.4. The PIV laser was arranged near transparent window made by glass on spiral case and the camera resolution is 15 frames. The PIV camera is fixed on the hydrostatic bearing and the camera is 50cm above the headcover, in Fig.4b. And the view area is on the observation window and is positioned by two bolt labeled by green circle, in Fig.4c. And the view area can include two impeller blades and three guide vane blades. The flow can be observed by the transparent windows.

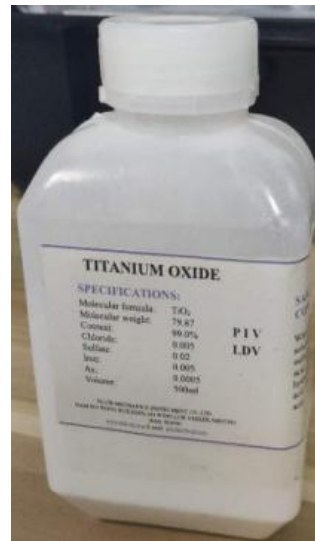
**2.3 PIV tracer particle**

PIV test shows that the selection of tracer particles is a very important to test results, and tracer particles should have good follow-ability and reflectance. A variety of tracer particles, mainly including silica, titanium dioxide and hollow glass beads are contrasted in the experimental, as shown in Fig.5. Through the comparison of

experimental results, it is finally determined that the hollow glass microspheres have the best test effect and can meet the requirements of the reflective and tracer particles.



(a) silica



(b) Titanium dioxide



(c) Hollow glass beads

**Fig. 5.** The PIV test tracer particle.

### 3 Results and analysis

#### 3.1 installation and debugging of field test devices

According to the test conditions of PIV, the platform and support for the laser, lens group, CCD camera and other test equipment with fixed PIV system are built.

1. Fix the laser so that it shines the laser light on the measured area (as shown in Fig. 6), and the laser height is located in the middle of the guide vane height.
2. Fix the CCD camera so that it can fully capture clearly the flow state of the measured window, as shown in Fig.6.



Fig. 6.The PIV laser on the middle of guide vane height.

#### 3.2 PIV test on pump hump condition

Take a pumped storage power station as an example: under the working condition of turbine, the rated head of the unit is 656m, the maximum head is 695m, and the minimum head is 626m. Under the working condition of pump, the maximum head of the unit is 711m, and the minimum head is 661m. The motor is a reversible synchronous motor with a rated capacity of 375MW and a speed of 500r/min. The model impeller of the power station is tested in the following working conditions. The tested working conditions include working point A,B,C,D,E, F and G.

The flow coefficient is defined

$$\varphi = \frac{4Q}{\pi D^2 u} \quad (1)$$

The pressure coefficient is defined

$$\psi = \frac{2gH}{u^2} \quad (2)$$

Where,  $Q$  is discharge,  $u$  is the average velocity at the outlet section,  $H$  is head,  $g$  is gravitational acceleration.

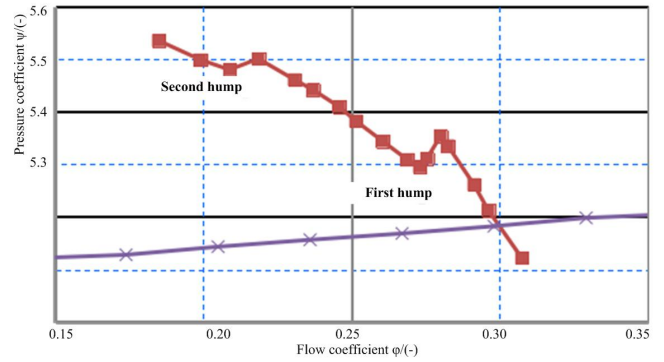


Fig. 7.The working points on pump  $H-Q$  curve.

The flow is shown on different working conditions in Fig.8. At working point A, the flow is very smooth at the location of the vane-less area. At working point B, the primary point of hump, the vortex begins to appear in the observation window. At working point C, the vortex develops fully and rotates clockwise and vortex cut off the ability of water from the runner flows to the guide vane. At working point D, the vortex develops fully and separates, and the hump gradually disappears. High-pressure water is free from the runner flows through the guide vane. The ability of pump water is regain. From the flow condition of the first hump, the first hump is closely related to the flow in the vane-less area between the guide vane and runner. It is the stall vortex in the vane-less area that induces the first hump.

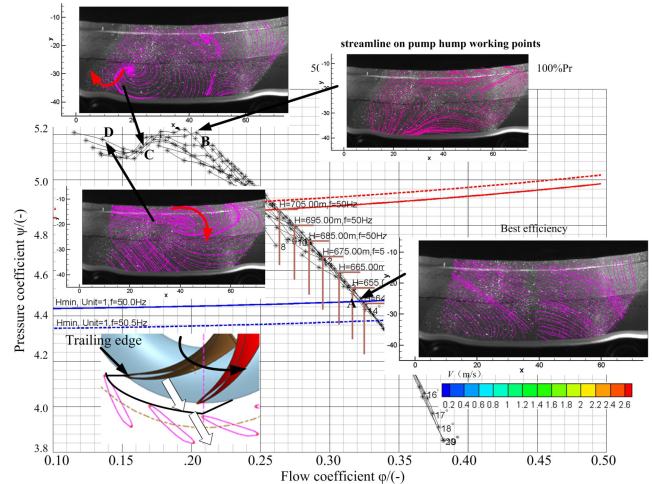


Fig. 8.The flow state on different working points on first hump of pump  $H-Q$  curve.

On the three working points E, F and G, second pump hump condition, the vortex is not obvious. On the vane-less area between guide vane and runner, the high pressure water is cross flow from runner to guide vane in Fig.9.

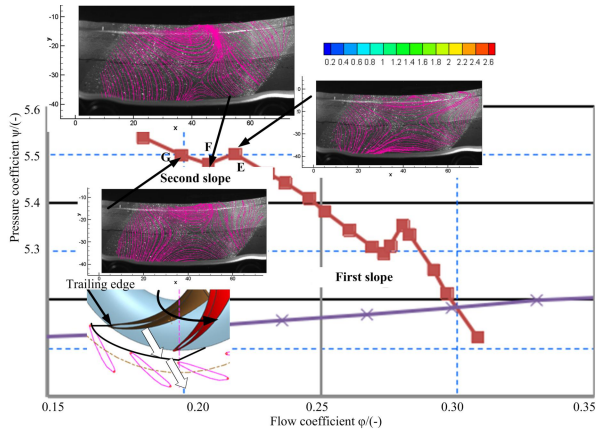


Fig. 9. The flow state on different working points on pump  $H-Q$  second hump curve.

From the second hump, the vortex distribution in the vane-less region is not obvious. Why the pump hump take place? With the help of CFD analysis, it can be found that there is a certain correlation between the second hump and the flow state at the runner leading edge in Fig.10. The shedding vortex is distribution along the runner leading edge.

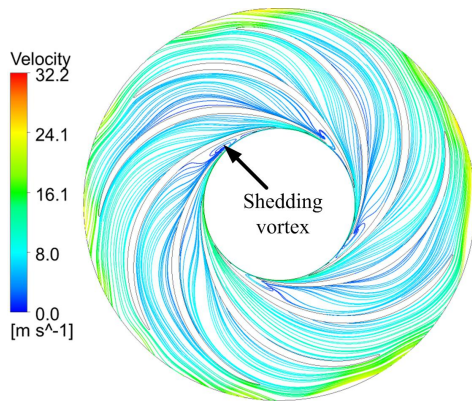


Fig. 10. The vortex distribution on runner leading edge of second hump of pump  $H-Q$  curve.

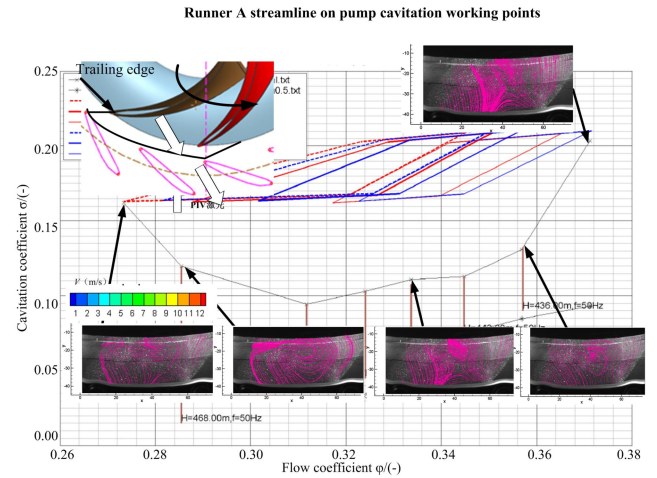
Comparing the flow field between first hump and second hump, the position of vortex initial is different. So the optimal measures are different. For the first hump, the optimal measures is the trailing edge of runner and the optimal measures is the leading edge for the second hump.

**3.3 PIV test on pump cavitation**

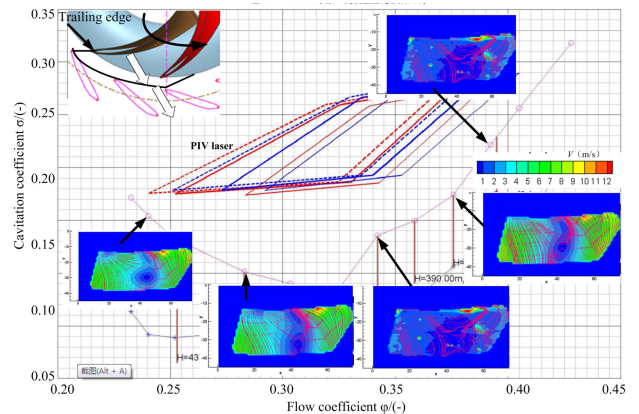
For the pump turbine, cavitation performance is an important index to ensure that the turbine does not have cavitation damage, and it is also an important index to ensure that the pump turbine does not have water column

separation. It is required that initial cavitation cannot occur in all working conditions, especially under plant cavitation coefficient. That means the initial cavitation coefficient curve can't interact with plant cavitation coefficient curve. In the Fig.11, comparing the runner A and B, the initial cavitation coefficient curve of runner A just is intersecting with plant cavitation curve and initial cavitation curve of runner B is smaller than the plant cavitation curve. That means the runner B can ensure the unite operates is full-wet state and runner A is full-dry state on the limited points.

By comparing the PIV test images of the two runners, it can be found that the distribution of vortices in the vane-less region of the two runners is quite different. The vortices in runner A are strong and well developed, while those in runner B are weak. The possible reason is that the initial cavitation of runner A changes the inlet flow Angle at the inlet of runner, and then changes the flow state at the outlet side of runner.



(a) Runner A cavitation curve and PIV picture



(b) Runner B cavitation curve and PIV picture

Fig.11. The PIV results on different initial cavitation working

points.

The distribution of cavitation is different at high and low heads. The cavitation bubbles at high head are concentrated on the suction surface and at low head on the pressure surface, in Fig. 12.

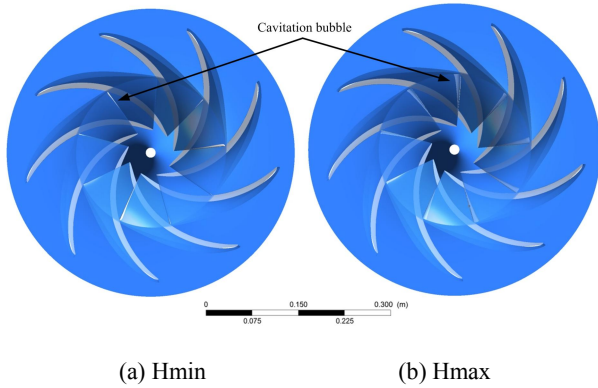


Fig.12. The cavitation bubble distribution on runner A. The white zone is cavitation bubble, which is 10% vapor volume fraction.

**3.4 PIV test on pump pressure fluctuation**

For the pump turbine, the pressure pulsation is the most serious in the turbine working condition, and the vane-less area is the position with the largest pressure pulsation amplitude. By comparing the different operating conditions in Fig.13, it can be found that the internal flow field varies greatly. In the optimal condition H, the flow in the vane-less region is smooth. At rated operating condition I, slight vortex separation has occurred. At 50% load condition J and no-load condition K, the vortex separation is already very serious. The vortices formed in the vane-less area seriously hinder the flow of water from the guide vanes to the runner, resulting in the accumulation of high-pressure water in the vane-less area. The pressure pulsation amplitude is very large in addition to the influence of rotor-stator interaction.

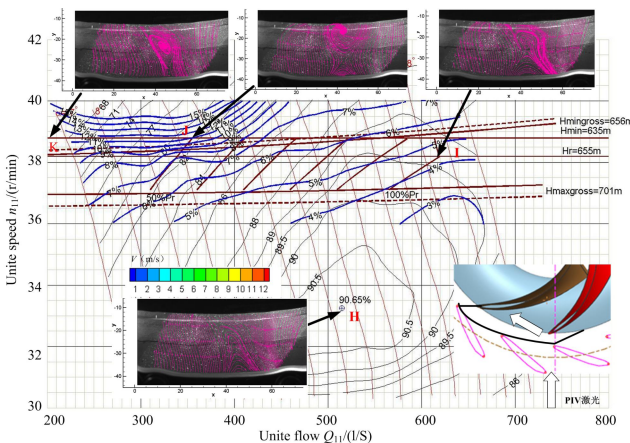


Fig.13. The PIV results on different pressure fluctuation working points.

**3.5 PIV test on four quadrants curve working points**

For pump turbines, operating conditions are often in constant conversion, such as pumping forward electricity, power generation phase modulation. In this series of

operating condition conversion process, the unit must run along the four-quadrant curve, so the four-quadrant curve is very important for the pump turbine. The shape of the four-quadrant curve directly determines whether the unit can realize the safe conversion between operating conditions.

For pump turbines, the four-quadrant curve shape of rated openness affects the safety of load rejection. PIV observations at the rated open characteristic operating conditions show that the flow characteristics at different operating conditions vary greatly.

PIV flow field observation was conducted at the characteristic working condition points on the rated guide vane opening 20°. In the reverse pump zone Q and the zero-flow condition R of the turbine, the vortices are serious. A vortex exists in the flow passage in the vane-less zone. As there is both flow in the direction of the turbine and the flow in the direction of the pump, the two flows cross each other. In S and L conditions close to the no-load condition, one vortex developed into a double vortex distribution. As the turbine and pump two-way flow rub each other. The bigger vortex is caused by the turbine direction of the flow induced and the smaller vortex is caused by the pump direction of the flow induced. The turbine flow is smooth with few vortices. In the braking condition M, the vortex strength gradually decreases. Close to the zero flow condition point N of the pump, the phenomenon of double vortices continues to appear. Pump operating conditions O and P, the flow is smooth in the channel. In the transition process, after the turbine load rejection, the unit's operating state from the turbine condition into no-load, no-load into the turbine brake, and then into the reverse pump area. From PIV test observation of internal flow field, it can be seen that from no load to the area where the reverse pump is located, strong vortices exist. Therefore, it is easy to understand that some units show the pressure exceeds the guaranteed value on volute and draft pipe during the transition process.

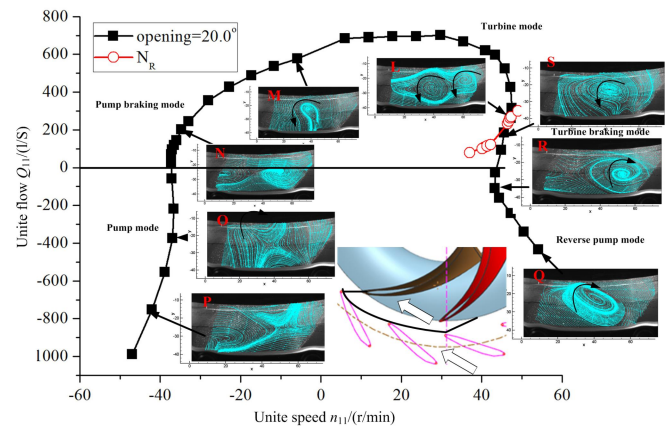


Fig.14. The PIV test results on guide vane opening 20°

For hump condition, cavitation condition, pressure pulsation and four-quadrant conditions, the common point

is that they all operate in deviation from the optimal conditions. Compared with the optimal condition, the velocity triangle changes in Fig.15. The flow angle also changed from  $\beta$  to  $\beta_5$ , which led to the separation of detached vortex. The macroscopic effect of these vortices is to produce these unstable phenomena.

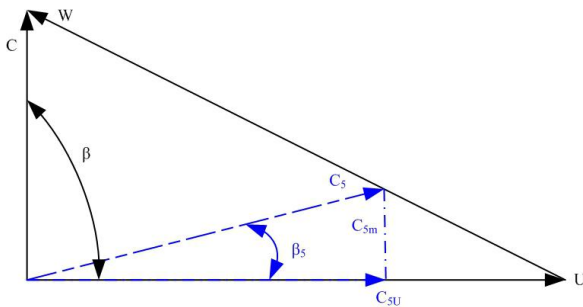


Fig.15. Velocity triangle (the solid line represents the optimal discharge, the dotted line represents the partial load working condition C5)

#### 4 Conclusions

In this paper, the flow field of the pump turbine is observed and studied by PIV. It mainly studies the unstable conditions of the pump turbine under the working conditions, such as the hump and cavitation conditions of the pump mode, the pressure pulsation conditions of the turbine and the four-quadrant conditions of the whole unit.

The following conclusions are obtained:

- (1) The flow states of the first hump and the second hump are quite different. The vortex separation area of the first hump occurs in the vane-less area, while the vortex separation of the second hump occurs at the leading edge of the runner.
- (2) The cavitation changes the inlet angle of the runner and the flow pattern at the outlet of the runner.
- (3) The amplitude of pressure pulsation is closely related to the vortex separation
- (4) The four-quadrant curve, especially the double vortices in no-load condition, seriously hindered the normal flow of water, resulting in excessive volute pressure and draft tube pressure.

#### Declarations

Availability of data and materials are true and tested by authors.

#### Competing interests

The authors declare that there is no conflict of interests regarding the publication of this paper.

#### Funding

The paper is supported by Deyang science and technology support program.

#### Authors' contributions

The author Liu demin is charge of the test research and author Zhao Yongzhi is incharge of pressure fluctuation and author Xu Weilin is incharge of paper revised.

#### Acknowledgements

The authors gratefully acknowledge the support from National Natural Science Foundation of China (No.51279172) and Deyang science and technology support program (2018CKJ002).

#### References

- [1] Annual development report of China's power industry[M]. Beijing: China building materials industry press[M], 2019.
- [2] ZUO Z G, LIU S H, SUN Y K, et al. Pressure Fluctuations in the Vaneless Space of High-Head Pump-Turbines-A Review[J]. Renewable and Sustainable Energy Reviews, 2015, 41(1): 965-974.
- [3] HASMATUCHI V, FARHAT M, ROTH S, et al. Experimental Evidence of Rotating Stall in a Pump-Turbine at Off-Design Conditions in Generating Mode[J]. Journal of Fluids Engineering, 2011, 133(5): 051104.
- [4] RAN H J, LUO X W. Experimental Study of Instability Characteristics in Pump Turbines[J]. Journal of Hydraulic Research, 2018, 56(6): 871-876.
- [5] XIA L S, CHENG Y G, ZHANG X X, et al. Numerical Analysis of Rotating Stall Instabilities of a Pump Turbine in Pump Mode[J]. IOP Conf. Series: Earth and Environmental Science, 2014, 22: 032020.
- [6] ZUO Z G, LIU S H. Flow-induced Instabilities in Pump-turbines in China[J]. Engineering, 2017, 3(4): 504-511.
- [7] EGUSQUIZA E, VALERO C, HUANG X X, et al. Failure Investigation of a Large Pump-Turbine Runner[J]. Engineering Failure Analysis, 2012, 23(7): 27-34
- [8] MIYABE M, FURUKAWA A, MAEDA H, et al. A Behavior of the Diffuser Rotating Stall in a Low Specific Speed Mixed-Flow Pump[J]. Turbomachinery, 2007, 35(2): 113-121
- [9] RAN Hongjuan, LUO Xianwu, ZHU Lei, et al. Experimental Study of the Pressure Fluctuations in a Pump Turbine at Large Partial Flow Conditions[J]. Chinese Journal of Mechanical Engineering, 2012, 25(6): 1205-1209.
- [10] Wang Z W and Zhou L J, 2001, Rotor stator interaction induced unsteady flow simulation, Journal of Tsinghua University (Sci & Tech), 41(10), 74-77.
- [11] Zobeiri A, Kueny J and Avellan F, 2006, Pump-turbine rotor-stator interactions in generating mode: pressure fluctuation in distributor channel, 23rd IAHR Symposium on Hydraulic Machinery and System, Yokohama.
- [12] Backman A G, 2008, CFD validation of pressure fluctuations in a pump turbine, Master Thesis, Lulea University of Technology, Sweden.
- [13] J P Yan, U Seidel and J Koutnik, 2012, Numerical simulation of hydrodynamics in a pump-turbine at off-design operating conditions in turbine mode, 26th IAHR Symposium on Hydraulic Machinery and System, Beijing.

- [14] Widmer C, Staubli T and Ledergerber N, 2011, Unstable characteristics and rotating stall in turbine brake operation of pump-turbines, *JFE*, 133, 041101.
- [15] Yin J L, Liu J T and Wang L Q, 2011, Prediction of pressure fluctuations of pump turbine under off design condition in pump mode, *Journal of Engineering Thermophysics*, 32(7), 1141-1144.
- [16] Xiao Y X, Sun D G and Wang Z W, 2012, Numerical analysis of unsteady flow behaviour and pressure pulsation in pump turbine with misaligned guide vanes, 26th IAHR Symposium on Hydraulic Machinery and System, Beijing.
- [17] Liu D M, Zheng J S and Shi Q H, 2012, Numerical simulation on the "S" characteristics and pressure fluctuation of reduced pump-turbine at start-up condition, 26th IAHR Symposium on Hydraulic Machinery and System, Beijing.

### Biographical notes

LIU Demin (Corresponding author), male, born in 1982, PhD, Post-doctoral, is currently a Senior Engineer at *Dongfang electric machinery company, China*. He received his doctor degree from fluid machinery Engineering, Tsinghua University, China, in 2011. His research interests include CFD and hydraulic design. He is in charge of Kaplan turbine, pump-turbine and all kinds of pumps. Especially he finished the Dunhua, Changlongshan, Panlong and Meizhou pump storage station pump-turbine unite design. He has published more than 30 papers.

Tel: +86-0838-2411953; E-mail: [liudemin999@126.com](mailto:liudemin999@126.com)

XU Weilin, male, born in 1963, PhD, professor, doctoral supervisor, "cheung kong scholars program" distinguished professor, *sichuan university*, hydraulics and the development and protection of state key laboratory of mountainous rivers, director of the State Council degree committee discipline appraisal group members, winners of national outstanding youth science fund, enjoy special government allowances of the State Council, the Ministry of Education science committee, academic and technical leaders of sichuan province, director of China water conservancy association. He has published more than 100 papers.

Tel: +86-028-85405915; E-mail: [xuwl@scu.edu.cn](mailto:xuwl@scu.edu.cn)

ZHAO Yongzhi, male, born in 1965, is currently a Senior Engineer at *Dongfang electric machinery company, China*. He received his master degree from fluid machinery Engineering, *Huazhong science University, China*, in 2001. His research interests include CFD and hydraulic design. He is in charge of Kaplan turbine and bulb turbine. He has published more than 10 papers.

Tel: +86-0838-2410038; E-mail: [zhaoyongzhi1965@126.com](mailto:zhaoyongzhi1965@126.com)

# Figures

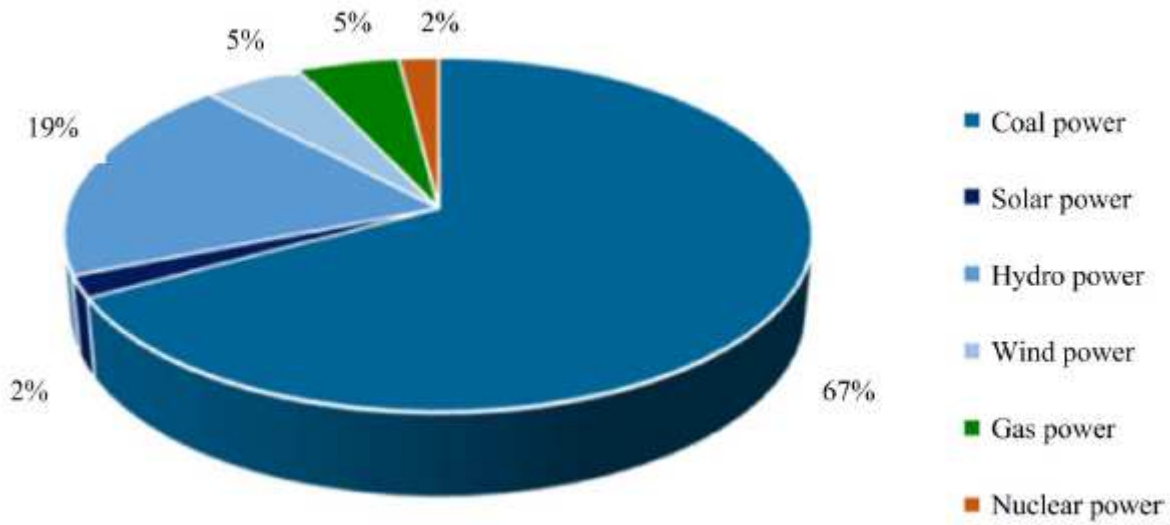


Figure 1

Ratios of different power generation in China

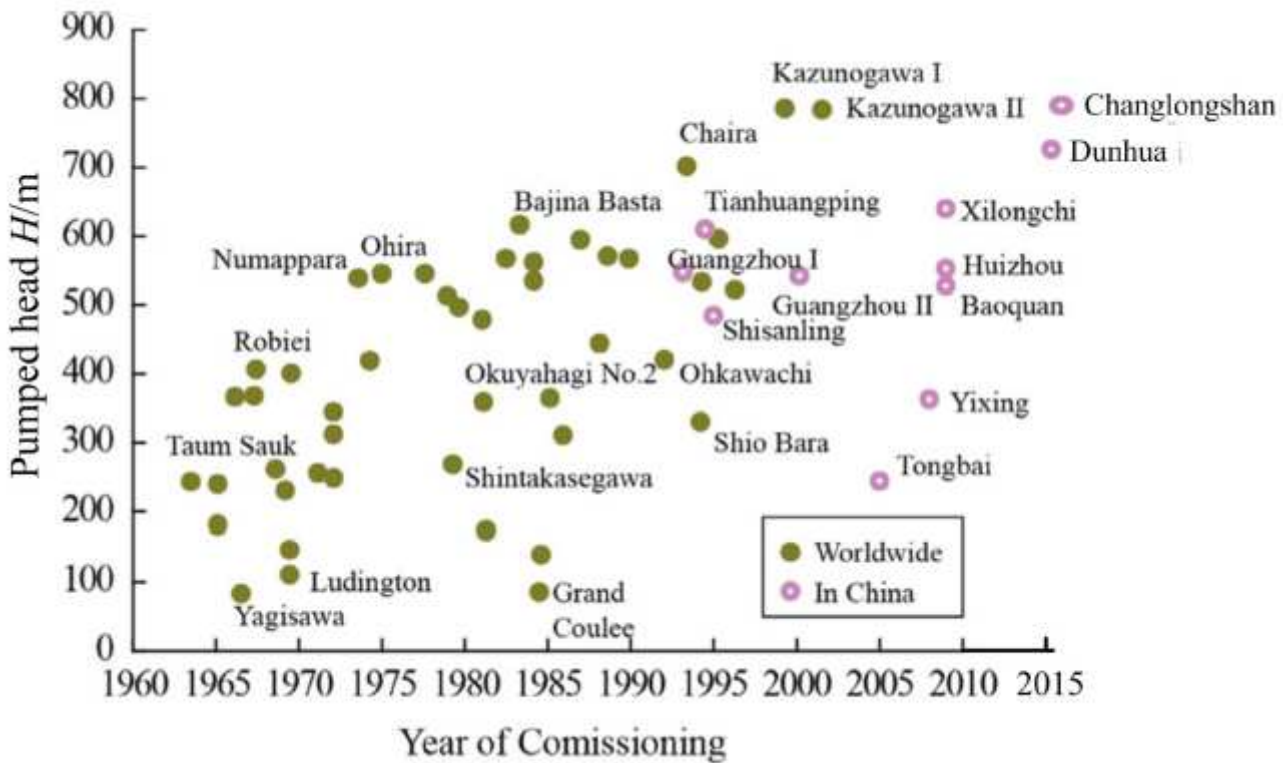


Figure 2

Pumping head variations for pumped storage power-stations[2]

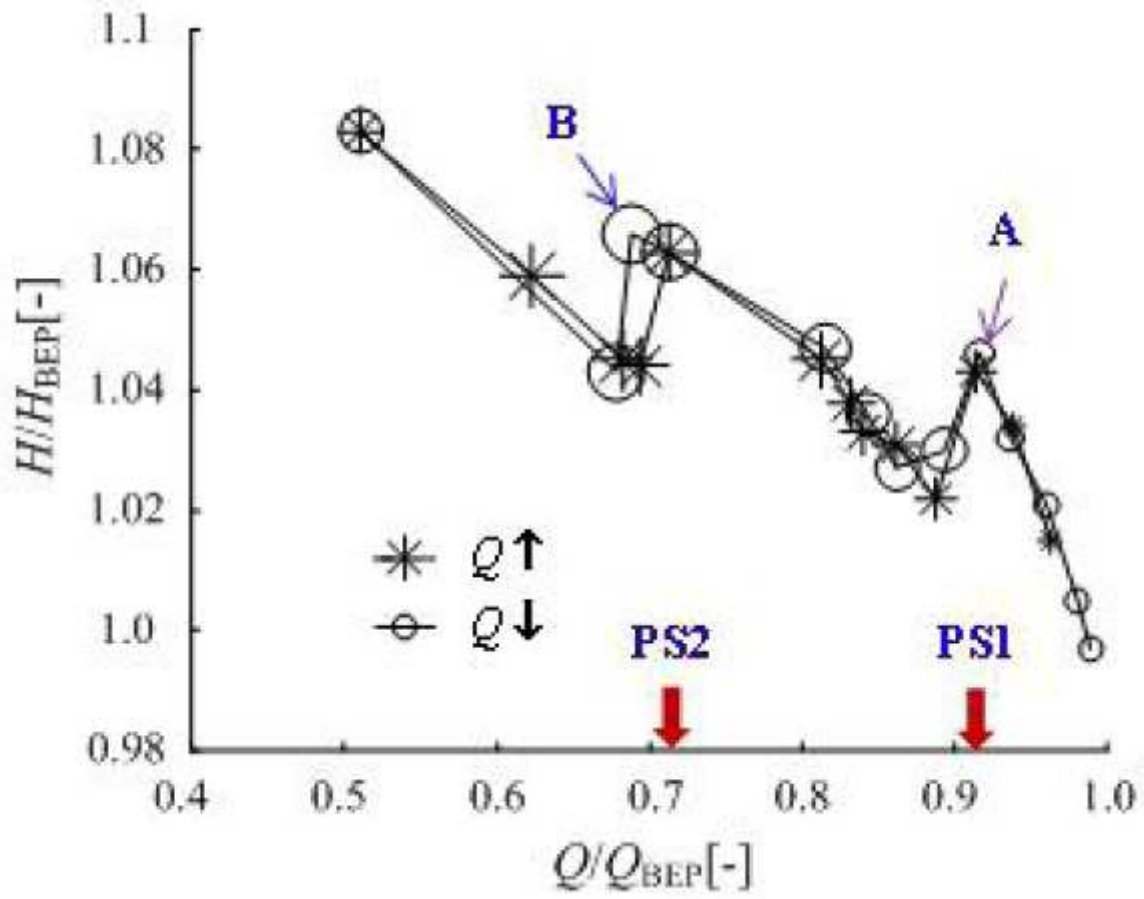
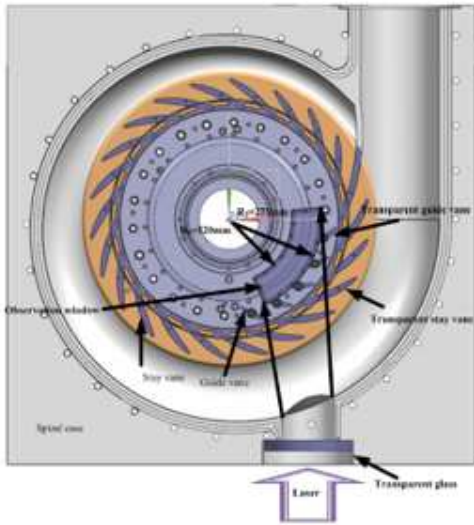


Figure 3

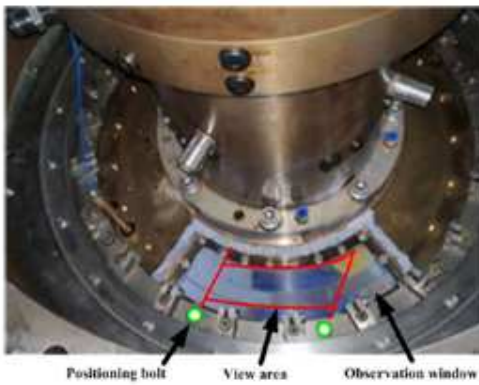
Positive slope at characteristic curve for pumped storage unit at pump mode



(a) Pump turbine structure for PIV test



(b) PIV camera



(c) Transparent window and view area

## Figure 4

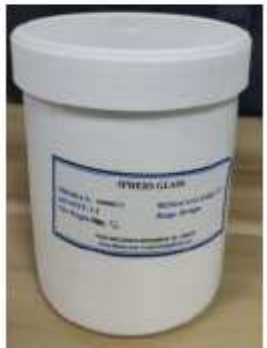
The structure of the pump-turbine model.



(a) silica



(b) Titanium dioxide



(c) Hollow glass beads

**Figure 5**

The PIV test tracer particle.



Figure 6

The PIV laser on the middle of guide vane height.

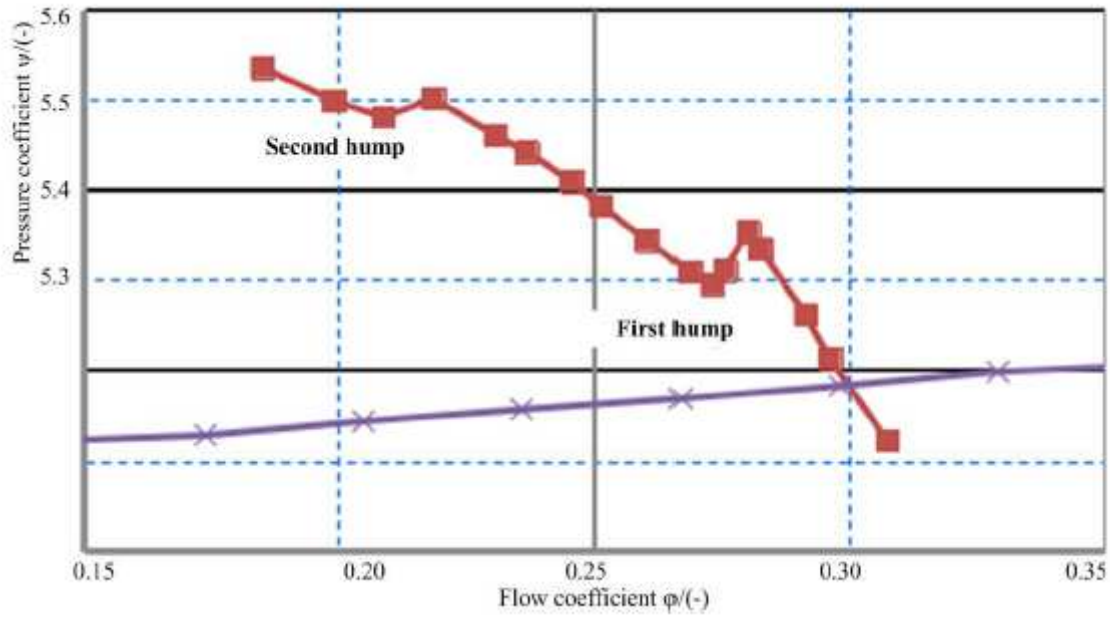


Figure 7

The working points on pump H-Q curve.

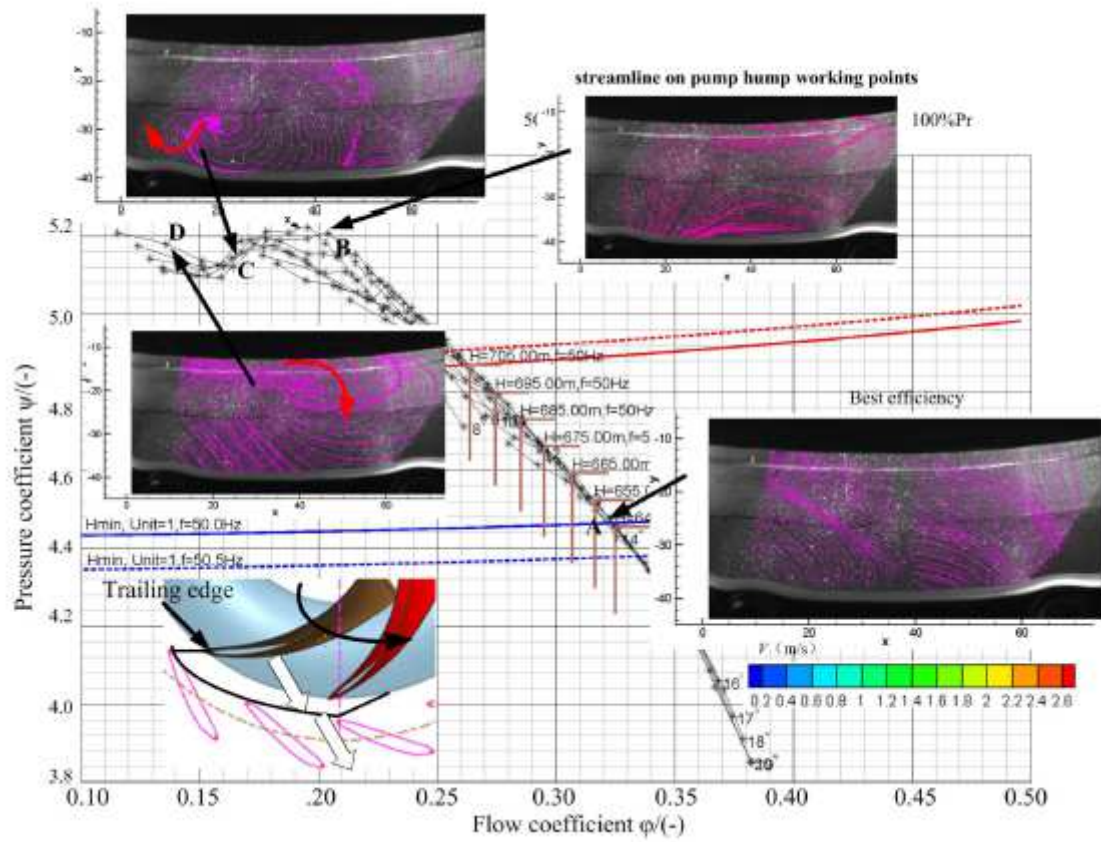


Figure 8

The flow state on different working points on first hump of pump H-Q curve.

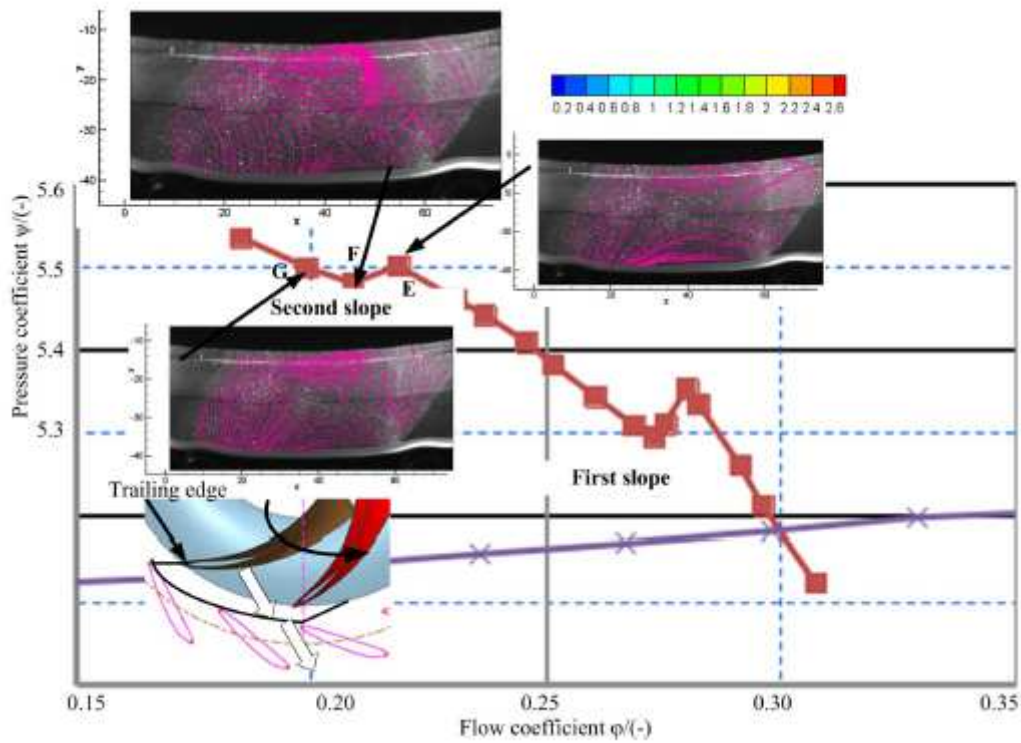


Figure 9

The flow state on different working points on pump H-Q second hump curve.

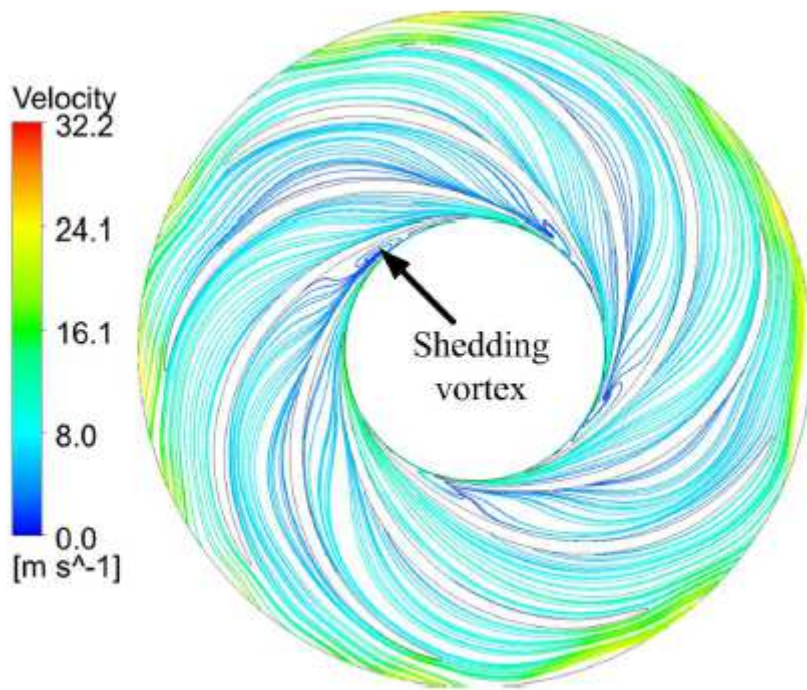
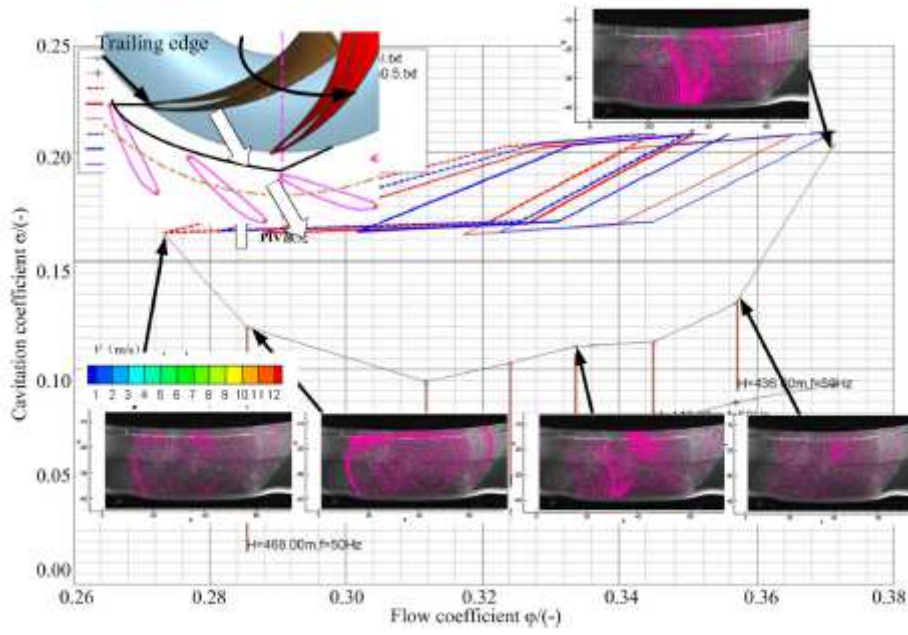


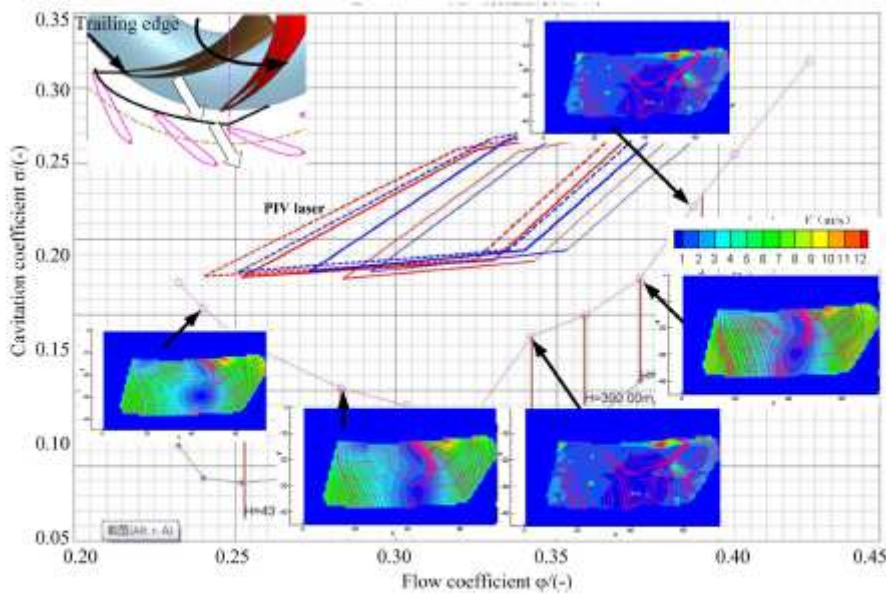
Figure 10

The vortex distribution on runner leading edge of second hump of pump H-Q curve.

Runner A streamline on pump cavitation working points



(a) Runner A cavitation curve and PIV picture



(b) Runner B cavitation curve and PIV picture

Figure 11

The PIV results on different initial cavitation working points.

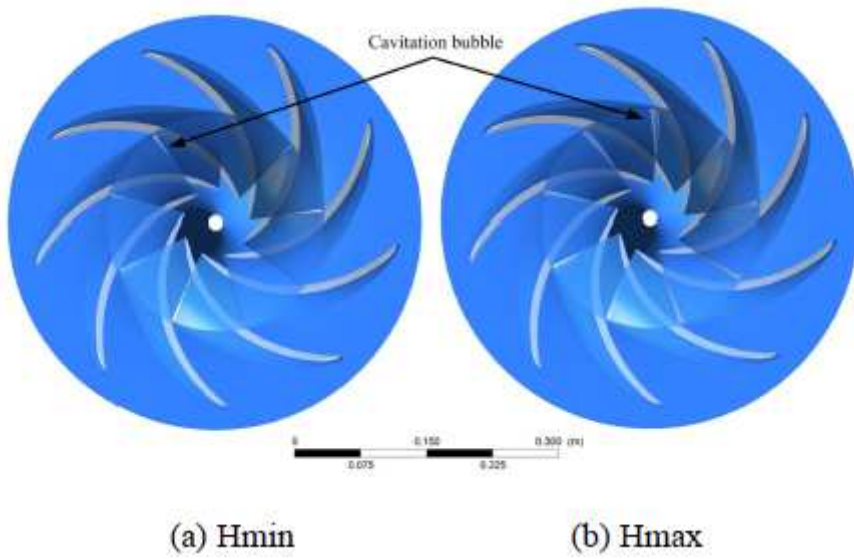


Figure 12

The cavitation bubble distribution on runner A. The white zone is cavitation bubble, which is 10% vapor volume fraction.

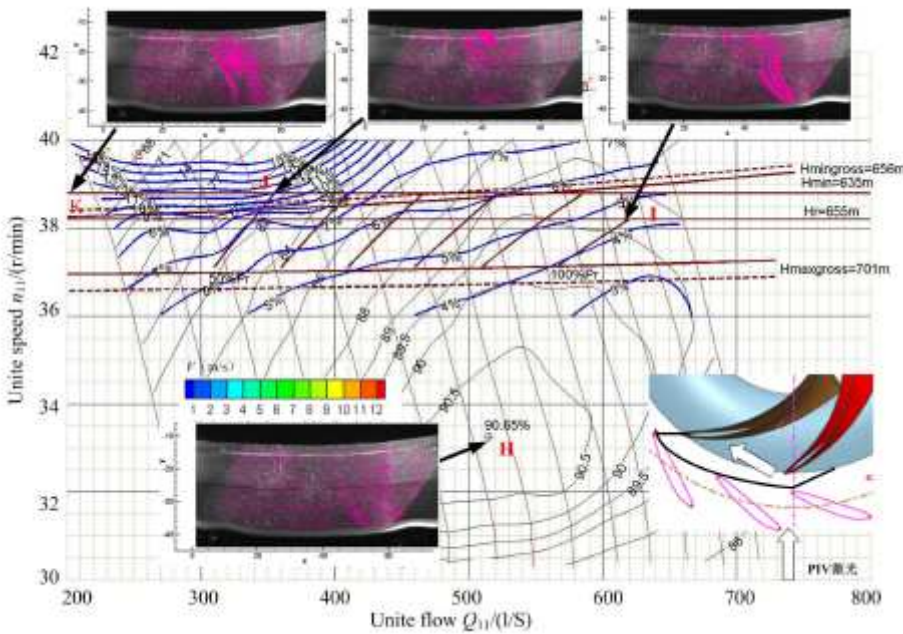


Figure 13

The PIV results on different pressure fluctuation working points.

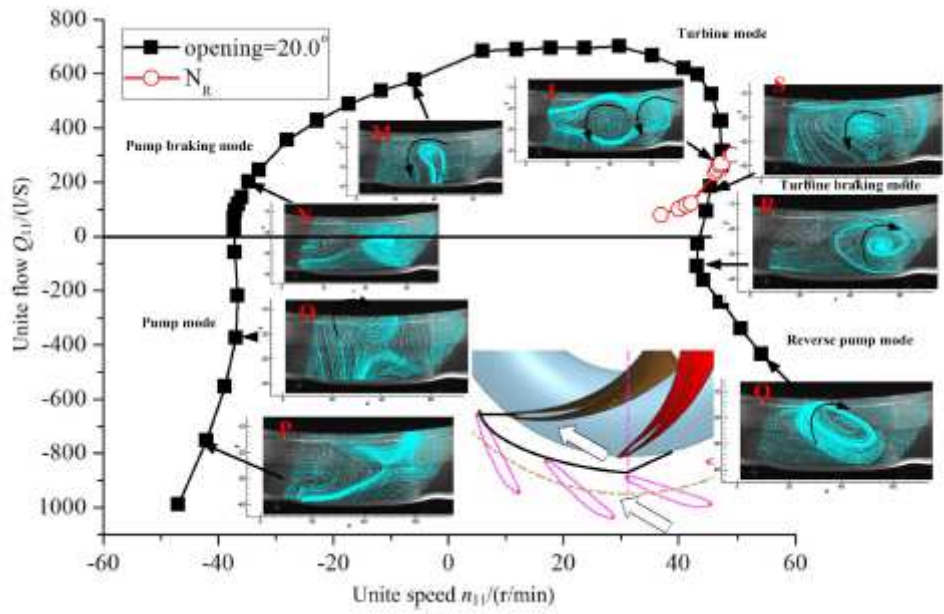


Figure 14

The PIV test results on guide vane opening 20o

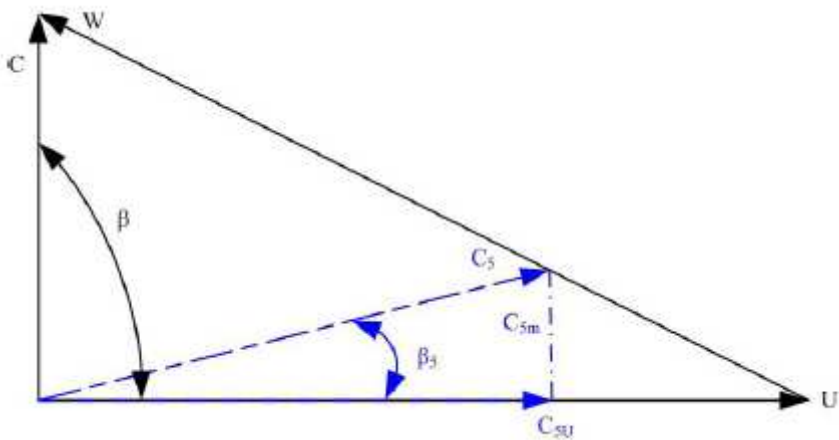


Figure 15

Velocity triangle (the sold line represents the optimal discharge, the dotted line represents the partial load working condition C5)